Intermediate states of GeO_2 glass under pressures up to 35 GPa

Xinguo Hong,[1] Guoyin Shen,[2] Vitali B. Prakapenka,[1] Matt Newville,[1] Mark L. Rivers,[1,3] and Stephen R. Sutton[1,3]
[1]*Consortium for Advanced Radiation Sources, University of Chicago, Chicago, Illinois 60637, USA*
[2]*HP-CAT, Carnegie Institution of Washington, Bldg 434E, Argonne, Illinois 60439, USA*
[3]*Department of Geophysical Sciences, University of Chicago, Chicago, Illinois 60637, USA*
(Received 19 December 2006; published 13 March 2007)

Density-driven polyamorphism of GeO_2 glass under high pressure has been studied by density, x-ray scattering, and optical Raman measurements. Density data obtained by an x-ray absorption method display distinct compression behavior in different pressure regions, with rapid density increases at 5 and 10 GPa and a plateau at 6–9 GPa. Simultaneous x-ray diffraction reveals that the position of the first sharp diffraction peak (FSDP) increases nearly linearly towards higher scattering vector with pressure up to 10 GPa. Both the width of the FSDP and the Raman stretching band of Ge-O-Ge (419 cm^{-1}) increase with pressure but exhibit changes in behavior at 2.5 and 7.5 GPa, indicating intermediate states exist in the glass before the collapse of local tetrahedral and pentahedral structural units, respectively. At pressures above 15 GPa, post-octahedral compression with progressive enhancement in network correlation is observed. The results indicate not only the discrete but also rotating intermediate states exist in GeO_2 glass under pressures up to 35 GPa.

DOI: 10.1103/PhysRevB.75.104201 PACS number(s): 61.43.Fs, 61.10.Ht, 64.70.Kb

I. INTRODUCTION

The term "polyamorphism" has been introduced to describe the existence of discrete amorphous structures in solid or liquid phases of the same chemical composition and the distinct structural transitions between these polymorphs.[1–4] Polyamorphism of the classic network-forming glasses such as GeO_2 and SiO_2 is of great interest because of industrial applications, Earth science implications[5] and significance in glass theory.[6]

At ambient pressure, the structures of GeO_2 or SiO_2 glass are dominated by tetrahedral GeO_4 or SiO_4 units. High pressure and temperature induce the formation of octahedral GeO_6 or SiO_6 units in the glass.[7–14] In volume-pressure space, the glasses collapse into the octahedral polyamorph within a narrow pressure range, showing a first-order-like phase transition.[3,7–9,14] However, some studies claim the same transformation is continuous.[15–18] Polyamorphism of GeO_2 glass is of particular interest because pentahedral units exist in the transition region based on the results of an *in situ* diffraction experiment[19] combined with extrapolated density data measured by the strain-gauge technique.[20] Molecular dynamics simulations suggests not a stable entire pentahedral but a mixture of four, five, and six coordinate state.[18]

Density of GeO_2 glass has been measured by optical,[9] strain-gauge,[20] Brillouin,[21] and ultrasonic techniques,[22] with, however, considerable discrepancies between these data at pressures above 5 GPa. The polyamorphic stability of GeO_2 glass, which is reflected by the equation of state (EOS), has been studied by optical methods to 7.1 GPa (Ref. 9) and strain-gauge techniques to 9 GPa,[20] covering approximately half of the coordination change region of 4–13 GPa defined by different techniques.[7–10] There is no evidence for the discrete pentahedral intermediate state in the existing density data, and the EOS of the octahedral form of the glass remains unknown. In fused quartz, sharp entropy-driven polyamorphous transition was observed at 3.6 GPa and 680 °C by direct density measurement,[14] while density-driven polyamorphous transition in SiO_2 glass occurs at much higher pressure of 10–25 GPa,[12] and there is no *in situ* density measurement reported so far.

Structure of GeO_2 glass exhibits interesting behavior under pressure. Permanently densified samples display significant changes in intermediate-range order (IRO) without change in local cation coordination.[23,24] Neutron and x-ray diffraction investigations show that this change in IRO is induced by the rotation of Ge-O-Ge bonds and distortion of the GeO_4 tetrahedra.[23,24] *In situ* diffraction experiments show large concurrent changes in IRO on the local coordination change.[19,25] Structural details of IRO related to pentahedral intermediate state or polyamorph remains to be clarified.

In this paper, we present results from *in situ* density measurements with diamond anvil cell (DAC), simultaneous x-ray diffraction, and Raman measurements to understand the fundamental compression process and the nature of polyamorphism in GeO_2 glass. The results indicate both discrete and rotating intermediate states in GeO_2 glass under different pressure regions up to 35 GPa.

II. EXPERIMENT

GeO_2 glass was prepared by placing the Pt capsule of GeO_2 power ~99.999%, Alfa Aesar, inside an oven at 1390 °C above melting point (1086 °C) for 12 h, followed by air quenching to room temperature. The amorphous structure was checked by x-ray diffraction and Raman scattering. We performed three kinds of experiments on the GeO_2 glass within the DAC at the GSECARS 13-BM-D and HPCAT 16-ID-B beamlines, Advanced Photon Source, Argonne National Laboratory. X-ray absorption and simultaneous angle-dispersive x-ray diffraction measurements were performed to determine the pressure dependence of density. Simultaneous x-ray diffraction measurements were also used to document structural transitions. *In situ* Raman measurements were made to investigate the pressure-induced structural correlation between tetrahedral structural units.

In the x-ray experiments, gem-quality single-crystal diamond anvils with large culet sizes of 500 and 800 μm were used to reduce pressure gradients and diamond deformation at sampling areas. Slotted WC seats were employed at both sides of DAC to ensure access to large angles (25°) for the incident and diffracted x-ray beams. GeO_2 glass was loaded without pressure-transmitting medium into an 80 μm diameter sample chamber in a preindented Mo and Re gasket of 40 μm in thickness for the DACs of 800 and 500 μm culet sizes, respectively. Pressures were determined using the pressure-dependent fluorescence of small ruby balls (<5 μm) scattered oppositely at the corner of sample chamber. The x-ray energies at 13-BM-D were 18.000 and 30.000 keV for x-ray absorption and simultaneous diffraction measurements.

At 13-BM-D, the x-ray beam size was focused down to 5(vertical) $\times$ 13(horizontal) μm at the full width at half maximum (FWHM) on sample by Kirkpatrick-Baez (KB) mirrors. The x-ray intensities before and after the DAC were monitored by an Ar-filled ion chamber and a photodiode, respectively. The x-ray diffraction and absorption measurements were performed at the sample center and the positions equidistant from the center 100 μm apart with acquiring time for about one minute to increase the signal-to-noise ratio. Additional x-ray diffraction experiments were carried out using intense monochromatic x-ray with a fixed energy at 29.210 keV at 16-ID-B to study the change of first sharp diffraction peak (FSDP).

The diffraction patterns of the samples and gaskets were recorded with a high-resolution Mar-345 IP area detector. Density of the crystalline Mo or Re gasket used for the calculation of sample thickness was obtained from the lattice parameters determined by fitting the observed diffraction peaks. X-ray absorption was measured at different angles of 0° and 20° to monitor and eliminate the influence of diamond diffraction. Details of density measurement with DAC can be found in our previous publication.[26] Analysis on the diamond curvature at high pressure was estimated by crystalline Ag as standard sample and will be published elsewhere.[27]

In Raman measurements, three DACs of gem-quality single-crystal diamond anvils with 300, 500, and 800 μm culet sizes were employed to measure the Raman shift of the main Ge-O-Ge stretching band (419 cm^{-1}). Raman scattering data were collected using the micro-Raman spectrometer at GSECARS (Spex 0.5 m monochromator and Princeton LN/CCD detector) using the 514.5 nm line of an Ar-ion laser and 20 μm focused laser spot in backscattering geometry.

III. RESULTS AND DISCUSSION

Densities of GeO_2 glass obtained from the x-ray absorption and simultaneous diffraction measurements up to 35 GPa are shown in Fig. 1. Density data displays little scatter with different DACs (squares and circles) and the variations in measurements at different angles are indicated by error bars. Density data exhibits distinct compression behaviors in different pressure regions. At low pressures the density from this method is consistent with the values from optical experiments[9] and the strain-gauge technique,[20] verify

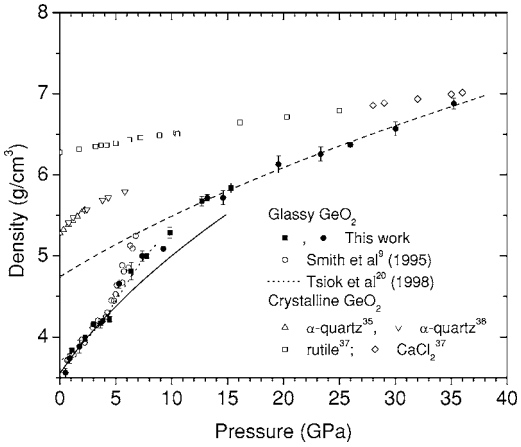

FIG. 1. Density of GeO_2 glass as a function of pressure determined with DACs of 500 μm culet size (solid circles) and 800 μm culet size (squares). For comparison, literature data are from Smith *et al.* (Ref. 9) and Tsiok *et al.* (Ref. 20). Crystalline phases: α quartz ($\triangle$, $\triangledown$);[35,36] rutile ($\square$) and $CaCl_2$ ($\diamond$).[37] Solid and dashed lines are the Birch-Murnaghan EOS for tetrahedral and octahedral forms, respectively.

the validity of present density measurement. In the tetrahedral glass below 4.4 GPa, there is a noticeable jump of 4% in density at 2.5 GPa and a plateau formed at 3.0–4.4 GPa. Upon the collapse of tetrahedral network indicated by diffraction and Raman measurements (see below), a rapid increase in density can be found at 4.4–6 GPa. Further increasing pressure shows a noticeable plateau at 6–9 GPa, followed by a quick increase in density from 9 to 13 GPa.

The ultimate stability limit of the tetrahedral framework can be estimated from its compression behavior. Equation of states of the tetrahedral and the octahedral coordinated forms are necessary for the judgments on the complement of octahedral transformation as well as the first-order transition in the glass at high pressure. The solid line in Fig. 1 represents a fit for the tetrahedral glass with the Birch-Murnaghan equation of state to the pressure-volume data below 4.4 GPa (calculated from the density). This gives $V_0=29.46$ cm^3, $K=11.6\pm1.5$ GPa assuming $K'=4$. The fitted V_0 is in excellent agreement with that from the optical technique.[9] Above 13 GPa the GeO_2 glass exhibits elastic behavior and the same fitting process gives $K=36.6\pm2.4$, $V_0=22.05\pm0.28$, with $K'=4$ for the octahedral form (dashed line, Fig. 1). The bulk modulus K for the octahedral form is nearly triple that of the tetrahedral form, while V_0 decreases by about 25%. Large anelastic behavior is observed in the present study at 5–13 GPa between the compression curves of the tetrahedral and octahedral forms. The so-called two-domain mechanisim[9] of GeO_4 and GeO_6 structure units is not observed. The distinct plateau at 6–9 GPa reveals the existence of a metastable intermediate state, consistent with previous neutron and x-ray observations.[19] From the compression of octahedral form, we can see that the transition to the octahedral form is nearly completed at 13 GPa.

In comparison with the densities of crystalline phases (Fig. 1), much larger compressibility of glassy GeO_2 is found over the entire pressure range to 35 GPa. The density of

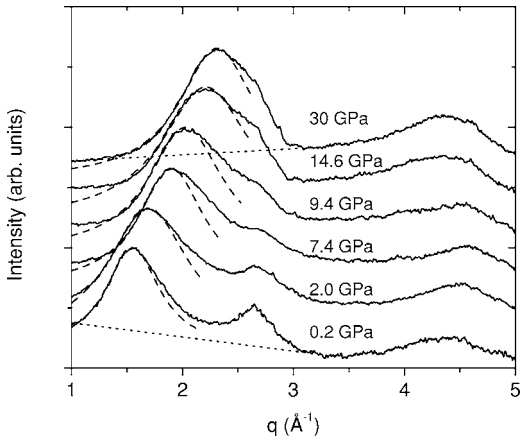

FIG. 2. *In situ* x-ray diffraction patterns of GeO_2 glass at high pressures. Each curve is shifted vertically for clarity. No background subtraction has been performed. The dashed lines show baselines that were subtracted to produce the FWHM data in Fig. 3.

glassy GeO_2 increases by a factor of 2, implying the cage contraction of the glass network plays an important role in the density-driven polyamorphism. The nature of IRO in the network glasses is usually characterized by the FSDP of the diffraction pattern, which reflects a finite number of periodic structural elements in the glass[6,28,29] and is associated with the cage or holes of the network in the glass.[30,31] Figure 2 shows representative *in situ* x-ray diffraction patterns of GeO_2 glass at 0.2, 2.0, 7.4, 9.4, 14.6, and 30 GPa. As pressure increases, the FSDP shifts towards higher scattering vector Q with changes in line shape and intensity, and finally merges with the second peak at 2.7 Å^{-1}. These observations agree well with previous x-ray measurements.[13,19,31]

The position of the FSDP, which is inversely related to periodicities in the real-space structure, can be determined accurately from the x-ray diffraction pattern fitted by the summation of a Lorentzian curve and a base line.[25] The fitting result is illustrated by the dashed lines in Fig. 2. The position of the FSDP Q_p determined by Lorentzian fitting [Fig. 3(a)] exhibits a nearly linear behavior with pressure up to 10 GPa. This linear behavior reflects the distinct reduction in the length scale of IRO, i.e., a continuous breakdown of IRO in the tetrahedral network upon compression. From the peak position alone, no clear evidence for an intermediate state could be seen. Because of the density retaining at 6–9 GPa, a reversely expanding process should take place in the local structure in order to compensate the density increase caused by the considerable shrinkage of network cages in this pressure region, as reported for GeO_2 (Refs. 7 and 19) and SiO_2.[32] At higher pressures up to 35 GPa, slight increases in the position of FSDP signifies the termination of marked contraction of the network cage or hole in the glass.

Figure 3(b) shows the peak width from the Lorentzian fitting of the FSDP (Ref. 25) (solid symbols). To overcome the influence of background, open circles in Fig. 3(b) show the full width at half maximum (FWHM) of the reduced FSDP by subtracting the tangential baseline starting from 1 Å^{-1}, where the coherent scattering intensity is low, toward the minimum at 3.5 Å^{-1}. The pressure dependence of the widths from these two methods is basically consistent. Both

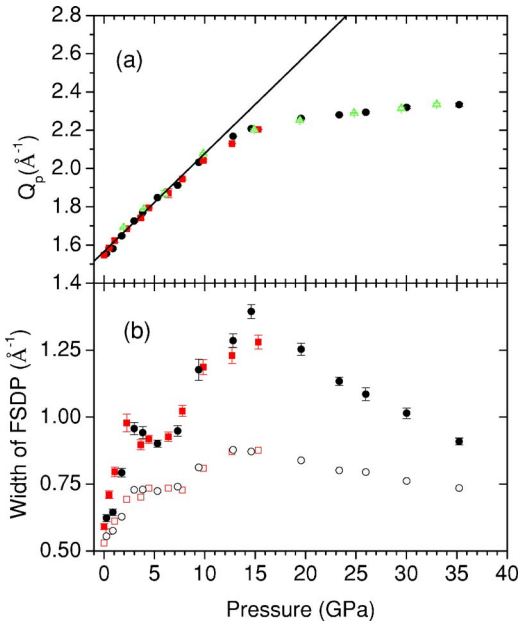

FIG. 3. (Color online) (a) Position of the FSDP of GeO_2 glass at high pressures (see text for details); (b) FWHM of the FSDP by direct Lorentzian fit to the FSDP (solid symbols) and that of the reduced FSDP by subtracting the baseline shown in Fig. 2 open symbols). DACs of 500 μm culet size (black solid circles and green up-triangles) and that of 800 μm culet size (red squares) were used.

methods show the width of the FSDP undergoes a dramatic evolution with increasing pressure. It broadens remarkably up to 2.5 GPa, but remains nearly constant up to 7.5 GPa, then further ascends to a crest at 15 GPa, and decreases continuously to 35 GPa. The anomalous point at 2.5 GPa is located noticeably earlier than the onset of density increase at 4.4 GPa, where the tetrahedral network collapses.[24] Another anomalous point at 7.5 GPa is just in the middle of the density plateau region at 6–9 GPa, prior to the formation of octahedra starting at 10 GPa.[19] This observation suggests that changes in IRO may be precursory and necessary for the local coordination transitions under high pressures. The maximum width of the FSDP at 15 GPa implies a minimum in the correlation length because the width of the FSDP Δq is inversely proportional to the correlation length R by $R=4\pi/\Delta q$. At pressures above 15 GPa, correlation length in the glass network is substantially enhanced. This suggests that the newly formed octrahedra at 15 GPa are weakly connected to each other. The minimum in correlation length is a sign of the emergence of a different compression mechanism in GeO_2 glass. With increasing pressures, the glass might change from a state, where is the concurrent presence of distorted edge-shared and corner-shared octahedra in the glass,[19] to more compact and perfect octahedral units in the glass.

To characterize pressure-induced line shape variation of the FSDP, the diffraction curves were reproduced using Gaussian model consisting three Gaussian peaks, denoted as GS-I, GS-II, and GS-III (Fig. 4). By free multipeaks fitting, the diffraction curves can be fitted well by three Gaussian peaks at low pressures, but only two Gaussian peaks is needed at pressures above 7.5 GPa, as shown by Fig. 4. Fig-

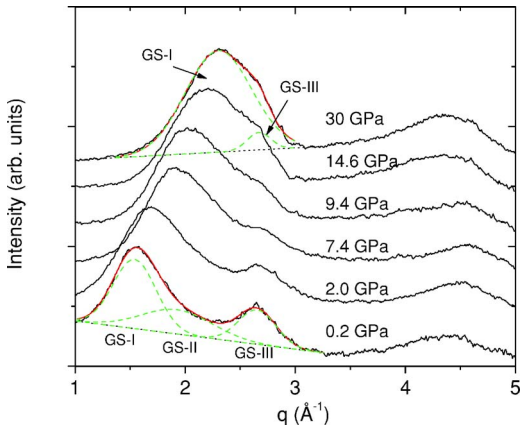

FIG. 4. (Color online) The FSDP together with the merging shoulder of in situ x-ray diffraction patterns of GeO_2 glass is reproduced using a Gaussian model [the red (dark gray) solid line] with three Gaussian peaks of GS-I, GS-II, and GS-III [the green (light gray) dashed line] and a tangential baseline starting from 1 Å^{-1} toward the minimum at 3.5 Å^{-1}. Each curve is shifted vertically for clarity.

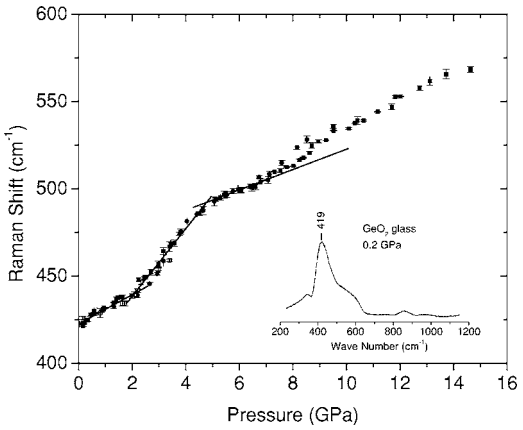

FIG. 6. *In situ* peak position of the 419 cm^{-1} Raman band of GeO_2 glass as a function of pressure to 15 GPa with DAC of 300 μm culet size (solid circles), 500 μm culet size (open squares), and 800 μm culet size (solid squares). The inset shows Raman spectrum of GeO_2 glass taken at 0.2 GPa. Solid line is from linear fitting below 2.1 GPa, while dashed and dotted lines from the fit at pressure region of [2.2,5] and [5,7], respectively.

ure 5 shows the optimized peak position of the Gaussian fit. The pressure dependence of GS-I peak position is essentially the same as that of FSDP [Fig. 3(a)], but discontinuities are observed for GS-II at 2.5 and 7.5 GPa, in accord with the width changes of FSDP [Fig. 3(b)]. A minimum at 9.5 GPa is found for GS-III.

The periodicities in the real-space structure can be estimated by $2\pi/Q_P$, where Q_P is the peak position, and at 0.2 GPa for GS-I, GS-II, and GS-III they are 4.1, 3.3, and 2.4 Å, respectively. The distance of 3.3 Å is close to the intertetrahedral Ge-Ge correlations at 3.2 Å between corner-shared tetrahedra. Distance of 2.4 Å arises either from O-O correlations or from the new Ge-O correlation formed by the approaching of the nearest-neighbor tetrahedron.[19] As increasing pressure to 2.5 GPa, all the peaks show gradual addition upon compression The jump of GS-II at 2.5 GPa should imply a discontinuity in intertetrahedral Ge-Ge correlations. At higher pressures, a distinct decrease in GS-III happens, forming a minimum at 10 GPa. This behavior agrees with the expanding process in O-O correlation as evident from the MD simulation.[19] The interrupt of GS-II in the pentahedral intermediate state reflects similar change in inter-pentahedral Ge-Ge correlations.

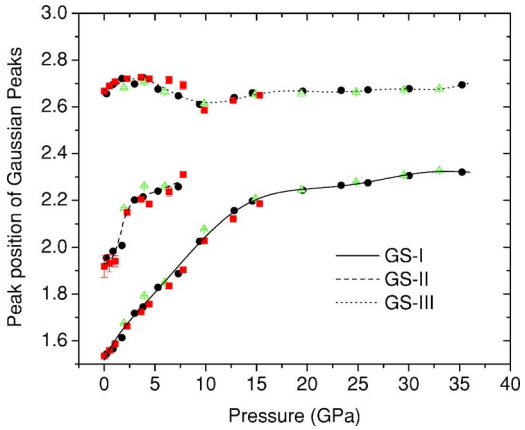

FIG. 5. (Color online) The optimized parameters of the Gaussian fit by GS-I, GS-II, and GS-III for FSDP. Symbols and colors are the same as Fig. 3. Spline lines are guides for eyes.

To further crosscheck our conclusions from the density and x-ray diffraction measurements, we performed Raman measurements with the results shown in Fig. 6. The inset shows the Raman spectrum of GeO_2 glass at 0.2 GPa, which is in good agreement with earlier Raman data of GeO_2 glass.[8] The strong 419 cm^{-1} band has been assigned to the symmetric stretching of bridging oxygens in a line bisecting the Ge-O-Ge plane in predominantly six-membered rings.[8,33,34] The shift of this Raman band to higher frequency is interpreted as an increase in distortion of GeO_4 tetrahedra and a decrease in the intertetrahedral bond angle.[8] Linear fit is used to highlight the distinct compression behavior in different pressure regions (Fig. 6). With initial compression up to 2.2 GPa, the main band shifts slowly to higher frequency, followed by a rapid shift up to 5 GPa. A slow shift is again observed in the region from 5 to 7 GPa, even though density rapidly changed and pentahedral units formed in this region. Another rapid increase to higher frequency is located at 7–8 GPa. These onset points of rapid shift in the stretching Ge-O-Ge (419 cm^{-1}) band basically coincide with the observations from the density and diffraction measurements, i.e., they occur earlier than the collapse of local tetrahedral and pentahedral units, respectively. These facts clearly indicate the presence of rotating intermediate states in GeO_2 glass before the coordination change in local structure.

IV. CONCLUSION

The above results lead to the following interpretation for the polyamorphism in GeO_2 glass. At pressures below 10 GPa, volume compression accompanied by a continuous

decrease in the cage size; before 2.5 GPa, the glass is constructed with a closer packing but little change in the dimensions of the individual GeO_4 tetrahedra,[7,8,24] from 2.5 to 4.4 GPa, an intermediate polymorph appears with little density change and rapid increase in Ge-O-Ge Raman shift, reflecting the deformation of GeO_4 tetrahedra. Further compression results in rapid increase in density due to the appearance of nonbonded oxygen atoms into the close proximity of the GeO_4 tetrahedra,[19] leading to the formation of discrete pentahedra in the glass and coordination number increase. The expansion of local structure compensates the cage shrinkage in the glass network and gives rise to the macroscopic density plateau at 6–9 GPa. With the newly formed pentahedra, a similar intermediate polymorph emerges at 7.5 GPa with little density variation and change in slope in the Ge-O-Ge Raman shift, reflecting the deformation of GeO_5 pentahedra. The entrance of additional nonbonded oxygen atoms into the first shell of Ge atoms produces the octahedral form in the glass, accompanied by other remarkable increases in density from 9 to 13 GPa. Above 15 GPa, the post-octahedral compression process is active.

ACKNOWLEDGMENTS

This work is supported by NSF-EAR Grant No. 0229987. The GSECARS sector is supported by the NSF (Earth Sciences Instrumentation and Facilities Program) and DOE (Geoscience Program). The HPCAT facility is supported by DOE-BES, NNSA_(CDAC)_, DOD-TACOM, and W. M. Keck Foundation.

[1] P. H. Poole, T. Grande, C. A. Angell, and P. F. McMillan, Science **275**, 322 (1997).
[2] V. V. Brazhkin and A. G. Lyapin, J. Phys.: Condens. Matter **15**, 6059 (2003).
[3] P. F. McMillan, J. Mater. Chem. **14**, 1506 (2004).
[4] S. K. Deb, M. Wilding, M. Somayazulu, and P. F. McMillan, Nature (London) **414**, 528 (2001).
[5] P. J. Heaney, *Silica, Physical Behavior, Geochemistry and Materials Applications* (Mineralogical Society of America, Washington, D.C., 1994).
[6] A. C. Wright, J. Non-Cryst. Solids **179**, 84 (1994).
[7] J. P. Itie, A. Polian, G. Calas, J. Petiau, A. Fontaine, and H. Tolentino, Phys. Rev. Lett. **63**, 398 (1989).
[8] D. J. Durben and G. H. Wolf, Phys. Rev. B **43**, 2355 (1991).
[9] K. H. Smith, E. Shero, A. Chizmeshya, and G. H. Wolf, J. Chem. Phys. **102**, 6851 (1995).
[10] M. Grimsditch, R. Bhadra, and Y. Meng, Phys. Rev. B **38**, 7836 (1988).
[11] M. Grimsditch, Phys. Rev. Lett. **52**, 2379 (1984).
[12] A. Polian and M. Grimsditch, Phys. Rev. B **41**, 6086 (1990).
[13] S. Susman, K. J. Volin, D. L. Price, M. Grimsditch, J. P. Rino, R. K. Kalia, P. Vashishta, G. Gwanmesia, Y. Wang, and R. C. Liebermann, Phys. Rev. B **43**, 1194 (1991).
[14] G. D. Mukherjee, S. N. Vaidya, and V. Sugandhi, Phys. Rev. Lett. **87**, 195501 (2001).
[15] M. Grimsditch, Phys. Rev. Lett. **52**, 2379 (1984).
[16] Q. Williams and R. Jeanloz, Science **239**, 902 (1988).
[17] P. V. Teredesai, D. T. Anderson, N. Hauser, K. Lantzky, and J. L. Yarger, Phys. Chem. Glasses **46**, 345 (2005).
[18] K. V. Shanavas, N. Garg, and S. M. Sharma, Phys. Rev. B **73**, 094120 (2006).
[19] M. Guthrie, C. A. Tulk, C. J. Benmore, J. Xu, J. L. Yarger, D. D. Klug, J. S. Tse, H.-k. Mao, and R. J. Hemley, Phys. Rev. Lett. **93**, 115502 (2004).
[20] O. B. Tsiok, V. V. Brazhkin, A. G. Lyapin, and L. G. Khvostantsev, Phys. Rev. Lett. **80**, 999 (1998).
[21] G. H. Wolf *et al.*, *High-Pressure Research: Application to Earth and Planetary Sciences* (American Geophysical Union, Washington, D.C., 1992).
[22] K. Suito *et al.*, *High-Pressure Research: Application to Earth and Planetary Sciences* (Ref. 21).
[23] C. E. Stone, A. C. Hannon, T. Ishihara, N. Kitamura, Y. Shirakawa, R. N. Sinclair, N. Umesaki, and A. C. Wright, J. Non-Cryst. Solids **293–295**, 769 (2001).
[24] S. Sampath, C. J. Benmore, K. M. Lantzky, J. Neuefeind, K. Leinenweber, D. L. Price, and J. L. Yarger, Phys. Rev. Lett. **90**, 115502 (2003).
[25] S. Sugai and A. Onodera, Phys. Rev. Lett. **77**, 4210 (1996).
[26] G. Shen, N. Sata, M. Newville, M. L. Rivers, and S. R. Sutton, Appl. Phys. Lett. **81**, 1411 (2002).
[27] X. Hong, G. Shen, and V. Prakapenka (unpublished).
[28] S. C. Moss and D. L. Price, *Physics of Disordered Materials* (Plenum Press, New York, 1985).
[29] D. L. Price, S. C. Moss, R. Reijers, M. L. Saboungi, and S. Susman, J. Phys.: Condens. Matter **1**, 1005 (1989).
[30] A. C. Wright, R. N. Sinclair, and A. J. Leadbetter, J. Non-Cryst. Solids **71**, 295 (1985).
[31] S. R. Elliott, Phys. Rev. Lett. **67**, 711 (1991).
[32] C. Meade, R. J. Hemley, and H. K. Mao, Phys. Rev. Lett. **69**, 1387 (1992).
[33] S. K. Sharma, D. Virgo, and I. Kushiro, J. Non-Cryst. Solids **33**, 235 (1979).
[34] F. L. Galeener, Phys. Rev. B **19**, 4292 (1979).
[35] J. D. Jorgensen, J. Appl. Phys. **49**, 5473 (1978).
[36] B. Houser, N. Alberding, R. Ingalls, and E. D. Crozier, Phys. Rev. B **37**, 6513 (1988).
[37] J. Haines, J. M. Lager, C. Chateau, and A. S. Pereira, Phys. Chem. Miner. **27**, 575 (2000).